

Functional consequences of mutations at the allosteric interface in hetero- and homo-hemoglobin tetramers

V. BAUDIN,¹ J. PAGNIER,¹ L. KIGER,¹ J. KISTER,¹ O. SCHAAD,² M.T. BIHOREAU,¹
N. LACAZE,¹ M.C. MARDEN,¹ S.J. EDELSTEIN,² AND C. POYART¹

¹ Institut National de la Santé et de la Recherche Médicale U 299, Hôpital de Bicêtre, 94275 Le Kremlin Bicêtre, France

² Département de Biochimie, Faculté des Sciences II, 30, quai Ernest-Ansermet, CH 1211 Geneva 4, Switzerland

(RECEIVED MARCH 24, 1993; REVISED MANUSCRIPT RECEIVED MAY 24, 1993)

Abstract

A seminal difference exists between the two types of chains that constitute the tetrameric hemoglobin in vertebrates. While α chains associate weakly into dimers, β chains self-associate into tightly assembled tetramers. While heterotetramers bind ligands cooperatively with moderate affinity, homotetramers bind ligands with high affinity and without cooperativity. These characteristics lead to the conclusion that the β_4 tetramer is frozen in a quaternary R-state resembling that of liganded HbA. X-ray diffraction studies of the liganded β_4 tetramers and molecular modeling calculations revealed several differences relative to the native heterotetramer at the "allosteric" interface ($\alpha_1\beta_2$ in HbA) and possibly at the origin of a large instability of the hypothetical deoxy T-state of the β_4 tetramer. We have studied natural and artificial Hb mutants at different sites in the β chains responsible for the T-state conformation in deoxy HbA with the view of restoring a low ligand affinity with heme-heme interaction in homotetramers. Functional studies have been performed for oxygen equilibrium binding and kinetics after flash photolysis of CO for both hetero- and homotetramers. Our conclusion is that the "allosteric" interface is so precisely tailored for maintaining the assembly between $\alpha\beta$ dimers that any change in the side chains of $\beta 40$ (C6), $\beta 99$ (G1), and $\beta 101$ (G3) involved in the interface results in increased R-state behavior. In the homotetramer, the mutations at these sites lead to the destabilization of the β_4 hemoglobin and the formation of lower affinity noncooperative monomers.

Keywords: β_4 tetramers; CO photodissociation; hemoglobin; molecular modeling; oxygen binding; site-directed mutagenesis

The hemoglobin (Hb) of vertebrates is composed of two pairs of α and β chains that have considerable homology in their sequences. All hemoglobin subunits or myoglobin in living species, from plants to higher vertebrates, fold in nearly the same tertiary structure (Fermi & Perutz, 1981; Dickerson & Geis, 1983). Nevertheless, a seminal difference exists between the two types of chains: isolated α chains associate weakly into dimers, whereas at the same concentration the β chains readily associate into tightly assembled tetramers. The self-association of β subunits into tetramers is favored by oxygenation, implying a higher ligand affinity for the tetramers than for the isolated chains (Valdes & Ackers, 1977). The β_4 tetramers are also stabilized at acidic pH (Turci & McDonald, 1983) and at high salt concentration (Tainsky & Edelstein,

1973). While heterotetramers bind ligands (oxygen or CO) at moderate affinity with high cooperativity, the β_4 tetramers bind ligands with high affinity without heme-heme interactions, resembling the properties of the R-state in $\alpha_2\beta_2$ tetramers or of the isolated α subunits (Antonini & Brunori, 1971). Finally, the reactivity of the sulfhydryl group at position $\beta 93$ is approximately the same in oxy or deoxy β_4 and in oxy hemoglobin, but is much decreased in deoxy hemoglobin. According to the stereochemical model proposed by Perutz (1970; Perutz et al., 1987), these characteristics suggest that the homotetramer β_4 is frozen in the high-affinity R quaternary structure (Monod et al., 1965).

X-ray diffraction studies of the CO form of the β_4 tetramer have confirmed the R-like quaternary structure of this Hb, with iron-iron atom distances indicating an almost exact 2,2,2 symmetry (Arnone & Briley, 1978). Crystal structure analyses of the β_4 tetramer revealed that, contrary to what is observed in most liganded hemo-

Reprint requests to: V. Baudin, Institut National de la Santé et de la Recherche Médicale U 299, Hôpital de Bicêtre, 94275 Le Kremlin Bicêtre, France.

globins, the C-terminal dipeptide of the CO β_4 tetramer was not disordered, but is firmly positioned by its interaction, via water molecules, with residues His 2 and Lys 132 of the sister β chain corresponding to the $\beta_1\beta_2$ interface in the normal heterotetramer (Arnone et al., 1982). Another major difference was found in the β_4 tetramer at residues located at the $\alpha_1\beta_2$ interface in hemoglobin that contribute to the allosteric transition between oxy and deoxy Hb tetramers. These authors reported that the side chain of β_4 Arg (C6) interacts with the side chain of β_99 Asp (G1) of the opposite β chain through a salt bridge that does not exist in oxy or deoxy HbA structures. This feature has been considered as a major determinant in the instability of the deoxy T-state conformation in the homotetramer because the replacement of the 41 Thr (C6) in the α chains by the bulky Arg residue "is not acceptable in the T-state." Unfortunately, crystals of deoxy β_4 tetramers suitable for diffraction studies have not yet been obtained. For this reason, the aim of the present work was to use natural mutation or site-directed mutagenesis to alter either the polarity or the size of certain residues at locations corresponding to the $\alpha_1\beta_2$ interface in reconstituted β_4 tetramers produced in *Escherichia coli*. Following the crystallographic analyses cited above and molecular modeling of the interface of interest, we have tested the influence of changing the residue at the β_4 Arg (C6), β_99 Asp (G1), and β_{101} Glu (G3) positions and compared the functional properties of hetero- and homotetramers resulting from these artificial mutations.

Results and discussion

Spectrophotometric studies of β subunits

Isolated β subunits readily associate into tightly assembled tetramers, with equal amounts of monomers and tetramers occurring near 10^{-6} M (Valdes & Ackers, 1978; Philo et al., 1988). The very high affinity of the isolated chains precluded any attempt to perform accurate oxygen equilibrium studies for subunit solutions with the instrumentation used for heterotetramers.

Figure 1A shows the static visible spectra and the difference spectrum ($\Delta\epsilon$, mM) between deoxy HbA and deoxy β_4 tetramer. This difference spectrum is similar in shape and amplitude to the kinetic difference spectrum reported by Antonini and Brunori (1971) between deoxy HbA (T-state) and the sum of equimolar solutions of isolated α and β deoxy subunits (R-state). Similar T – R visible spectra have also been reported by Perutz et al. (1974) for deoxy spectra with or without inositol hexabiphosphate (IHP) of various high oxygen affinity hemoglobins. This observation supports the view that the unliganded β_4 tetramer is in an R-like structure (deoxy R or R_0) (Monod et al., 1965; Arnone et al., 1982). Figure 1B illustrates the spectra of CO HbA (R-state) and CO β_4 tetramer (R' -state) and their difference spectrum.

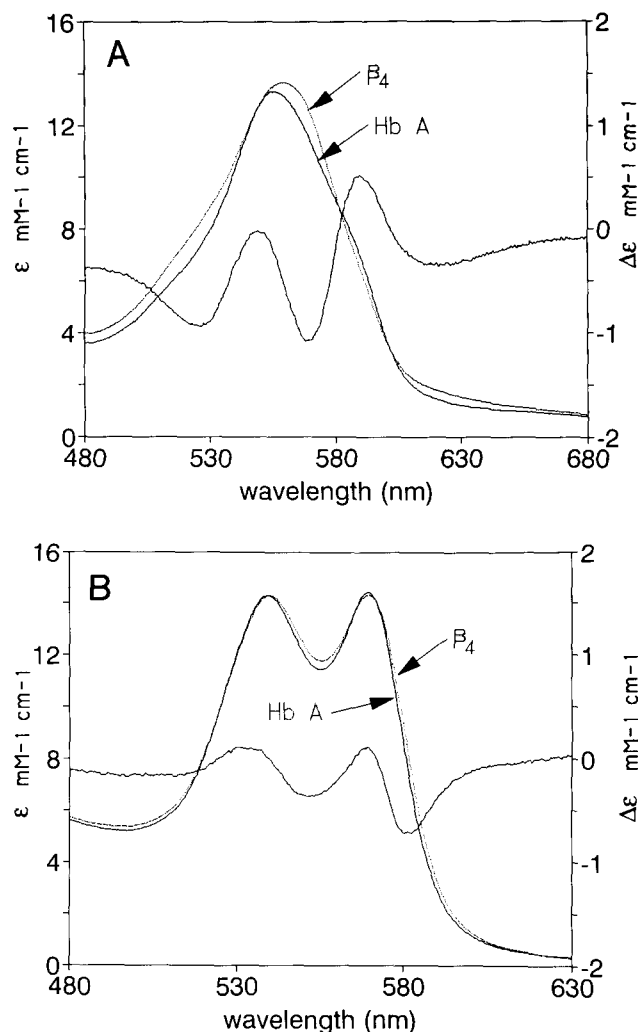


Fig. 1. Static visible spectra for HbA and β_4 tetramer in the deoxy (A) and carbon monoxide forms (B). The figure also shows the difference spectra between HbA – β_4 subunits of the deoxy and liganded compounds. The absolute spectra for the two species were recorded with the SLM DW 2000 spectrophotometer. Absorbance values were converted to millimolar extinction coefficients (ϵ , mM⁻¹ cm⁻¹). Heme concentration was determined in CO saturated solutions with $\epsilon_{568.5\text{nm}} = 14.3$ (Zijlstra et al., 1991). Conditions were 0.1 M NaCl, 50 mM Tris buffer, 1 mM EDTA, pH 7.2, 25 °C. Heme concentration was approximately 110–120 μ M. Optical pathlength was 0.2 cm.

A small red shift of the β_4 tetramer spectrum relative to that of COHbA was observed. The difference spectrum between CO HbA – CO β_4 is similar to that reported by Philo et al. (1981) between concentrated (high affinity) – diluted (lower affinity) liganded β chain solutions. On the basis of these experiments performed in different laboratories, it is difficult to establish a straightforward correlation between the liganded spectra of the heme complexes and their ligand affinity. Analysis of these spectra does suggest, however, that the tertiary configuration of the β hemes in the β_4 tetramers is not the same as that of the β hemes in the heterotetramer. Apparently the absence of

the α subunits is sufficient to produce the difference spectrum. The origin of the differences in ligand affinity and spectra between β monomers and tetramers is still unknown. One may conclude that any solution of isolated β chains is made of a mixture of low affinity monomers and high affinity tetramers, whose relative proportion depends mainly on the heme concentration and to some extent to various physicochemical factors such as pH and ionic strength (Tainsky & Edelstein, 1973; Kurtz et al., 1981; Turci & McDonald, 1983; Philo et al., 1988).

In order to better investigate the functional properties of the hemes in the β_4 tetramer, we have recorded the faint absorbance band III existing only in the static deoxy spectrum of HbA at about 760 nm and compared it with that in β_4 deoxy tetramer. A shift to higher wavelengths of band III with increased ligand affinity in various heme complexes has been observed (Kiger et al., in prep.). This inhomogeneous broadened absorption band reflects the large distribution in the population of the five coordinated high spin ferrous hemes. This band has been assigned to a charge transfer between the porphyrin π -system and the iron ($a_{2u}(\pi) \rightarrow dyz$) (Eaton et al., 1978) and was used by different authors as a probe of static and kinetic tertiary structural changes in the vicinity of the heme (Friedman, 1985). Recently Dunn and Simon (1991) studied the kinetics of the band III changes appearing after photodissociation of CO HbA. They showed that 35 ps after the light pulse, a transient spectrum was observed with a band maximum located at 765 nm, i.e., red shifted by almost 6 nm relative to the deoxy HbA band III. This transient remained unchanged up to 60 ns, indicating that the geometry of the heme group is only partly relaxed and that equilibration of the surrounding protein structure occurs on a longer time scale (Sawicki & Gibson, 1976; Martin et al., 1983; Petrich et al., 1991). Figure 2 shows the equilibrium characteristics of band III in the deoxy HbA (maximum absorbance at 760 nm) compared to that of the deoxy β_4 tetramer, which is red shifted infrared by almost 6 nm, i.e., at nearly the same wavelength as the 35 ps transient reported by Dunn and Simon (1991) after photodissociation of CO HbA. Kinetic hole burning experiments by Campbell et al. (1987) indicated that the most red shifted wavelength species were associated with the faster recombining population (higher ligand affinity) of the photoproducts. These results have been interpreted as indicating an incomplete relaxation of the Fe/heme geometry after the flash, in which the deoxy iron is not totally in the heme plane (presumably between its position in the T_0 and R_4 conformations) and the proximal histidine is maintained in its upright position (R_4 position). Although the similarity of the absorption bands III between unliganded β_4 tetramer and deoxy HbA at 35 ps may be fortuitous, we postulate here that they reveal similar conformations of the hemes. Accordingly, the results for the β_4 tetramer may indicate that the deliganded β hemes do not make a transition to the

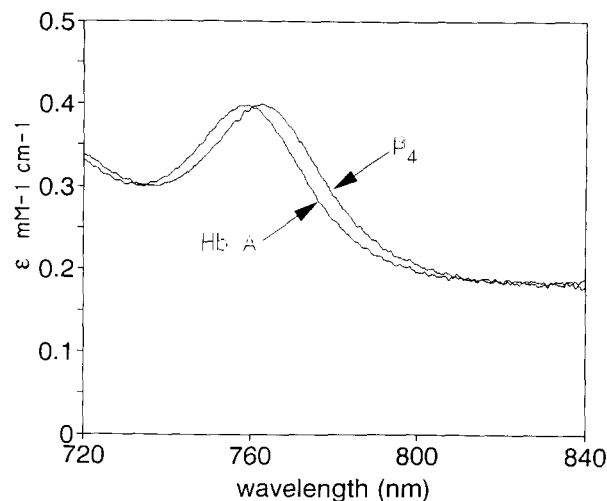


Fig. 2. Absorption band III in deoxy HbA and deoxy β_4 tetramers. Experimental conditions were as described for Figure 1. In both samples, small amounts of a buffered sodium dithionite solution were added to the deoxygenated hemoglobin solutions to remove remaining traces of oxygen and to reduce a small percentage of methemoglobin. These optical spectra were calculated after subtraction of the small absorbance spectra of the CO complexes and are therefore plotted as $\Delta\epsilon$ ($\text{cm}^{-1} \text{mM}^{-1}$) vs. wavelength.

tense T-state, as observed in the heterologous tetramer. They are rather in an "R-state" conformation similar to that observed at 35 ps in HbA by Dunn and Simon (1991), consistent with the high ligand affinity of the hemes in the homotetramers. The spectrophotometric studies described above suggest that the R_0 states are similar for HbA (as a photoproduct) and for β_4 at equilibrium; we postulate that the explanation for the homotetramer being frozen in an " R_0 -state" may be due to a stabilization of the R structure or more likely to a large destabilization of the unliganded T-state. Support for this hypothesis is given by the UV Raman resonance spectra of Kitagawa (1992), who showed that deoxy β_4 tetramers exhibit the larger shift of the $\nu_{\text{Fe-His}}$ frequency (224 cm^{-1}), still higher than that measured in mutant hemoglobins in which the increased ligand affinity is attributed to the large destabilization of the T quaternary structure.

Oxygen equilibrium studies of tetrameric Hb variants at the $\alpha_1\beta_2$ interface

Mutations at the $\beta 40$ (C6) position

In native Hb, the $\beta 40$ (C6) residue is arginine. This residue is a major participant in the $\alpha_1\beta_2$ "flexible joint" region, which contributes significantly to heme-heme interaction. Two natural mutants have been discovered at this position: Hb Waco (Arg \rightarrow Lys) (Mrad et al., 1989) and Hb Austin (Arg \rightarrow Ser) (Moo-Penn et al., 1977). We have engineered three additional mutations: Arg \rightarrow Ala,

Table 1. Oxygen binding parameters for $\alpha_2\beta_240$ Hb variants^a

	$\beta 40$ Arg	$\beta 40$ Lys ^b	$\beta 40$ Ser ^c	$\beta 40$ Ala	$\beta 40$ Asp
P_{50}	5.1	4.1	2.2	2.2	1.2
n_{50}	2.7	2.1	2.0	1.6	1.0
Bohr effect ^d	-0.5	-0.3	Normal	nd	nd
DPG effect ^e	0.5	0.4	Normal	0.4	nd
IHP effect ^f	1.0	0.9	Slightly decreased	0.7	0.15

^a P_{50} (in mm Hg) is the partial pressure of oxygen for half saturation; n_{50} is the Hill coefficient at half saturation. Experimental conditions: pH 7.2, 0.1 M NaCl, 50 mM bisTris, 20 μ g/mL catalase, 50 μ M EDTA, 60–80 μ M heme, 25 °C.

^b The measurements were performed on the hemolysate of a β^0 thalassemia/Hb Waco-Athens-Georgia patient (Mrad et al., 1989).

^c Values are from Moo-Penn et al. (1977).

^d $\Delta \log P_{50}/\Delta \text{pH}$.

^e $\Delta \log P_{50}$, ± 1 mM DPG.

^f $\Delta \log P_{50}$, ± 1 mM IHP.

Val, and Asp. Oxygen binding results for the mutants $\beta 40$ Arg \rightarrow Ala and Arg \rightarrow Asp are given in Tables 1 and 2 and in Figure 3. As expected from the similarity in size and charge, substitution of Arg by Lys in native Hb Waco does not affect its oxygen binding properties to an appreciable extent. However, this substitution does produce a lower n_{50} value and slightly diminished heterotropic effects (Bohr, sodium 2,3-diphosphoglycerate [DPG], and IHP effects) relative to native HbA. When Arg is replaced by Ser at the $\beta 40$ (C6) position, the oxygen affinity is in-

Table 2. Allosteric parameters for $\alpha_2\beta_240$ Hb variants^a

Hb	L	c	K_R	K_T	$\%T_3$	i_s
Hb $\beta 40$ Arg	1.1×10^5	0.0087	0.27	31.0	6.7	2.45
Hb $\beta 40$ Lys	3.8×10^4	0.0252	0.27	10.7	37.4	2.86
Hb $\beta 40$ Ala	3.8×10^3	0.0668	0.26	3.9	59.4	3.13
Hb $\beta 40$ Asp	1.0	1.0	1.2	—	—	—
+1 mM DPG						
Hb $\beta 40$ Arg	4.8×10^5	0.0090	0.48	53.3	25.9	2.78
Hb $\beta 40$ Lys	3.2×10^5	0.0164	0.40	10.7	58.1	3.0
Hb $\beta 40$ Ala	3.3×10^4	0.0352	0.34	9.7	59.0	3.11
+1 mM IHP						
Hb $\beta 40$ Arg	2.1×10^6	0.0131	1.00	76.3	82.5	3.36
Hb $\beta 40$ Lys	8.3×10^5	0.0183	1.00	54.6	83.7	3.41
Hb $\beta 40$ Ala	2.3×10^5	0.0233	0.46	19.7	74.4	3.28
Hb $\beta 40$ Asp	2.1	0.4400	1.33	3.0	15.2	0.90

^a The allosteric parameters (L , K_R , and K_T) were obtained after fitting the experimental curves to the equation of the two-state allosteric model by using a nonlinear least-square procedure. K_R and K_T (mm Hg) are the equilibrium oxygen dissociation constants for the R- and T-states, respectively; L is the allosteric constant ($=T_0/R_0$); c is K_R/K_T ; i_s , the switchover point, was calculated as $-\log L/\log c$. $\%T_3$ is the amount of triply liganded T-state species calculated as $(Lc^i)/(1+Lc^i)$ with $i = 3$. Experimental conditions were pH 7.2, 100 mM NaCl, 25 °C.

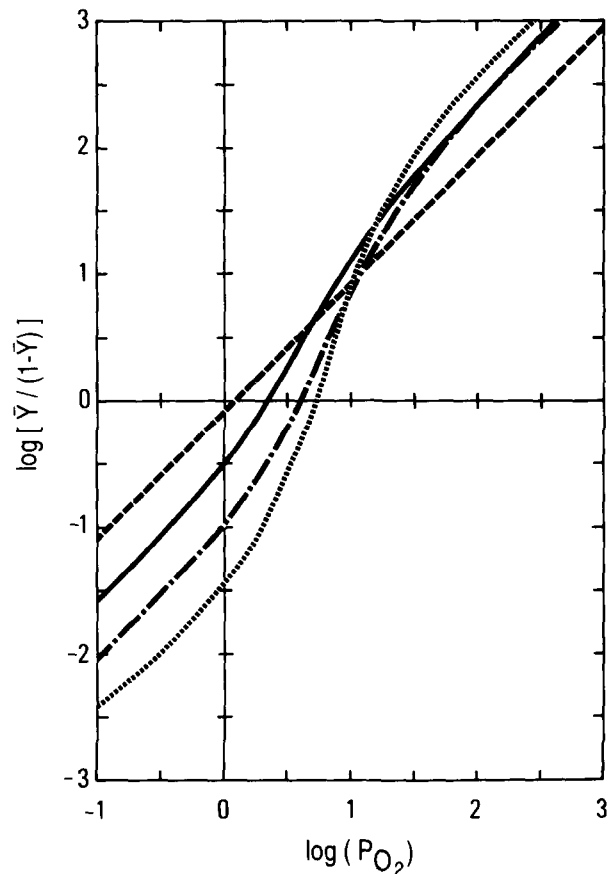


Fig. 3. Oxygen equilibrium binding curves (Hill plots) for the $\alpha_2\beta_240$ Hb variants described in the text. From right to left: (.....) HbA $\alpha_2\beta_240$ (C6) Arg; (—○) $\beta 40$ Arg \rightarrow Lys; (—□) $\beta 40$ Arg \rightarrow Ala; (---) $\beta 40$ Arg \rightarrow Asp. Conditions of the measurements were pH 7.2, 50 mM bis-Tris, 0.1 M NaCl, 25 °C. Hemoglobin concentration were approximately 60 μ M on a heme basis. Experimental curves were fit to the equation of the two-state allosteric model using the parameters given in Tables 1 and 2 (Kister et al., 1987).

creased twofold, with a low n_{50} value, while the heterotropic effects are normal or slightly decreased. This indicates that the principal properties of the “switch region” and the organophosphate binding site are maintained in this Hb. The authors of the study have reported a high tendency for this mutant to form dimers, which may account in part for the low n_{50} value and increased oxygen affinity (Moo-Penn et al., 1977). The artificial Hb $\beta 40$ Arg \rightarrow Ala synthesized in *E. coli* exhibits functional properties similar to those of Hb Austin, i.e., a marked increase in oxygen affinity and decreased cooperativity. Substitution of the negatively charged Asp residue for the positively charged Arg leads to a dramatic increase in oxygen affinity and elimination of heme-heme interaction. These changes are not reversed upon addition of IHP, indicating a serious destabilization of the deoxy quaternary structure for this mutant. As a whole, the data for this series of mutants show that any variation at the Arg po-

Table 3. Oxygen binding parameters for $\alpha_2\beta_2101$ Hb variants^a

	$\beta101$ Glu	$\beta101$ Gln	$\beta101$ Ala	$\beta101$ Lys	$\beta101$ Asp	$\beta101$ Gly
P_{50}	5.1	5.7	3.4	2.5	0.9	0.8
n_{50}	2.7	2.4	2.2	2.2	1.9	1.6
Bohr effect	-0.5	-0.55	-0.45	Normal	Normal	Normal
DPG effect	0.5	0.4	0.4	0.5	0.4	0.4
IHP effect	1.0	1.0	nd	1.0	0.85	0.95

^a P_{50} , n_{50} , and experimental conditions as in Table 1. The β mutant hemoglobins have been described as: β Glu \rightarrow Gln, Hb Rush; β Glu \rightarrow Lys, Hb British Columbia; β Glu \rightarrow Asp, Hb Potomac; β Glu \rightarrow Gly, Hb Alberta (Shih et al., 1985); β Glu \rightarrow Ala (*E. coli*, this study).

sition—due to change in either size (Ser), hydrophobicity (Val or Ala), or charge (Lys, Asp)—influences the oxygen binding properties while maintaining heterotropic effects close to normal. One should point out that the Arg \rightarrow Asp substitution leads to a complete destabilization of the T structure and to enhanced dimer formation, as demonstrated by high performance size-exclusion chromatography (not shown).

Mutations at the $\beta101$ (G3) position

Mutations at the $\beta101$ (G3) Glu position also lead to profound alterations of the oxygen binding properties of the mutated Hbs (IHIC, 1992). Tables 3 and 4 present the results of oxygen binding studies for the available natural mutants (Shih et al., 1985). In addition, we have synthesized the $\beta101$ (G3) Glu \rightarrow Ala to test for the consequences of the replacement of the negatively charged Glu by the small hydrophobic Ala residue, which should not result in creating a cavity or act as a helix breaker as Gly may do in Hb Alberta. Overall, these results lead to the following conclusions: (1) Suppressing the negative charges of the $\beta101$ residue in Hb Rush (Glu \rightarrow Gln) results in a slight decrease in oxygen affinity and a moderately increased Bohr effect, which was attributed to an extra chloride binding site (Shih et al., 1985). (2) For all other mutants listed in Table 3, increased oxygen affinity and decreased cooperativity are observed. (3) All mutated Hbs in this series exhibit normal or close to normal effects of the heterotropic cofactors. (4) Suppression of

one aliphatic carbon in the negatively charged Asp in place of Glu is sufficient to produce a very high oxygen affinity with low cooperativity but with a normal Bohr effect and normal interactions with organic phosphates. (5) Substitution of $\beta101$ (G3) Glu by either Gly or Asp results in comparable alterations of the functional properties of Hb.

Mutations at the $\beta99$ (G1) position

Drastic changes in oxygen binding properties of Hb are observed after substitutions at the $\beta99$ (G1) Asp site. This residue is involved in the crucial hydrogen bond with α chain residues that stabilize considerably the T structure at the $\alpha_1\beta_2$ interface. All seven natural hemoglobin mutants discovered at this position (IHIC, 1992) exhibit a high oxygen affinity and low cooperativity in ligand binding, but only slight modifications of their interactions with the heterotropic effectors. This suggests the increased tendency to form dimers in the deoxy form, which may be reassembled into tetramers upon addition of the effectors.

The present results can be described globally in terms of the original mechanistic model of Perutz (1970). Liganded tetramers have nearly the same affinity as dimers or isolated chains. The oxy R-state was thus described as “relaxed,” meaning that there is no induced stress due to tetramerization. Because in the R-state the subunit-subunit interactions are weak, it is reasonable that perturbations of the “allosteric” interface do not change the R-state affinity. However, in the T-state, the deoxy hemes somehow pull against each other. In this tense state, slight structural changes might cause the entire system to slip or even break. The latter appears to be true for the mutant $\alpha_2\beta_240$ (C6) Arg \rightarrow Asp, where there is nearly complete loss of the T-state properties. The change is less drastic for the mutant $\alpha_2\beta_240$ (C6) Arg \rightarrow Ala, whose properties appear to be due to a decrease in the “tension” of the T-state. It seems that the T-state has “slipped” toward a more “relaxed” state. This results in a compensated effect, with a T'-state exhibiting an increased affinity for oxygen. However, because this T'-state is now energetically closer to the R-state, addition of ligands has a smaller effect

Table 4. Allosteric parameters for $\alpha_2\beta_2101$ Hb variants^a

Hb	L	c	K_R	K_T	$\%T_3$	i_s
HbA	1.1×10^5	0.0087	0.27	31.3	6.7	2.45
Hb $\beta101$ Ala	2.2×10^4	0.0344	0.25	7.3	47.2	2.97
+1 mM DPG						
HbA	4.8×10^5	0.0090	0.48	53.3	25.9	2.78
Hb $\beta101$ Ala	3.1×10^5	0.0166	0.35	9.7	58.6	3.09

^a Definitions and conditions as in Table 2.

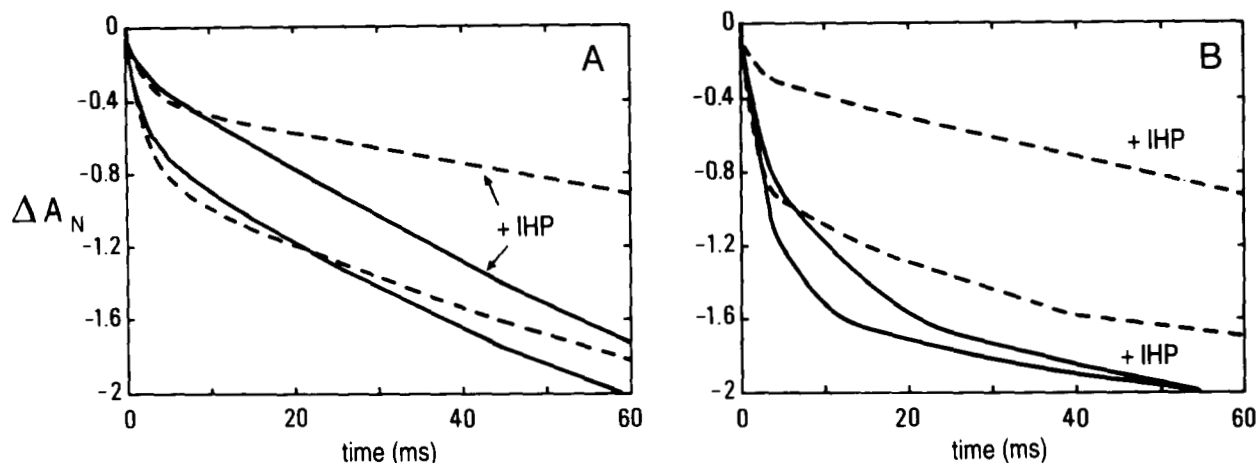


Fig. 4. Kinetics of CO bimolecular recombination to mutant $\alpha_2\beta_240(C6)$ Arg \rightarrow Ala (**A**) and to $\alpha_2\beta_240(C6)$ Arg \rightarrow Asp (**B**). The solid curves are for the mutated Hbs; the dashed curves are for control HbA. Conditions were 40% photodissociation, 0.1 atm [CO], pH 7.2, 0.1 M NaCl. Buffered IHP (0.5 mM, pH 7.2) was added as indicated. Hemoglobin concentration was approximately 100 μ M on a heme basis. Optical pathlength was 0.1 cm. The vertical axis is the log of the normalized change in absorption.

(larger c) on the allosteric equilibrium. There is thus more of the T'-state (50% T₃ for the mutant vs. 7% for HbA), which compensates the higher T' affinity, leading to a change in P_{50} that is smaller than that of K_T (Tables 2, 4).

Kinetics of CO recombination to native and *E. coli* synthesized $\alpha_2\beta_2$ tetramers

CO bimolecular recombination kinetics after flash photolysis of the heterologous hemoglobin $\alpha_2\beta_240(C6)$ Arg \rightarrow Ala and $\alpha_2\beta_240(C6)$ Arg \rightarrow Asp are illustrated in Figure 4. While the fast initial rate corresponding to CO bimolecular recombination to the mutants' quaternary R-state is similar to that found for normal HbA, we observed a 1.5-fold increase in the (slow) T-state on-rate for the Arg \rightarrow Ala mutation with more T-state behavior (23% vs. 15% for normal HbA). Addition of the allosteric effector IHP to the Arg \rightarrow Ala mutant results in an increase of the T-state kinetic phase comparable to the increase observed in HbA. Similar results were obtained for the Arg \rightarrow Val mutation (not shown). By contrast, flash photolysis of the CO Arg \rightarrow Asp mutant leads to nearly monophasic R-state recombination kinetics, which are barely influenced upon addition of IHP. These results are in agreement with the oxygen equilibrium results for this mutant, and indicate that introduction of a negatively charged Asp residue at position C6 of the β chains leads to the disruption of the normal contacts at the $\alpha_1\beta_2$ interface. We have also engineered the $\beta 101(G3)$ Glu \rightarrow Ala, whose equilibrium oxygen binding indices are given in Tables 3 and 4. Kinetics of CO recombination for this synthetic mutant display an increased T-state on-rate, compatible with a higher affinity for the ligand (Fig. 5).

Kinetics of CO recombination to mutant β_4 tetramers

It has been suggested by Kurtz and Bauer (1978) and Valdes and Ackers (1978) that the oxygenated β subunits self-associate into tetramers more strongly than do the deoxy subunits. These data imply that the oxygen affinity of β_4 should be higher than that of β monomers. In contrast to the behavior of oxy β , photodissociation of CO- β solutions gives rise to rebinding kinetics that are biphasic (Philo et al., 1988). In every case, at least two exponentials are required to fit the CO kinetic data. Simu-

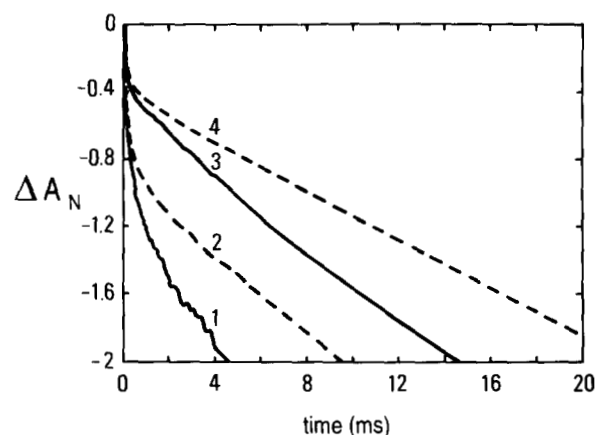


Fig. 5. Bimolecular recombination kinetics of CO to 100 μ M solution of the $\alpha_2\beta_2101(G3)$ Glu \rightarrow Ala mutant in the absence (1) and presence (3) of 0.5 mM IHP compared to native HbA (2 and 4, dashed lines) at pH 7.2, 0.1 M NaCl, 50 mM bisTris, 40% photodissociation, 0.1 atm [CO].

lations consistently show two phases differing in rate by a factor of 3–4, with the relative proportion of the faster phase increasing at higher protein concentrations. These data are consistent with a concentration-dependent equilibrium between tetramers and monomers. Under our experimental conditions, the fit for the recombination kinetics of CO to 100 μM solutions of β chains indicates 85% fast phase (corresponding to tetramers) of rate $12 \times 10^6 \text{ M}^{-1} \text{ s}^{-1}$, while at 0.5 μM β chains, we obtained 65% slow phase with a rate of $3 \times 10^6 \text{ M}^{-1} \text{ s}^{-1}$. These values agree with those published by Antonini and Brunori (1971) and Philo et al. (1981). For β_{PMB} subunits that are predominantly monomeric at all concentrations, curve fitting gave 92% slow phase.

Because our analyses did not reveal a dependence of the rate of CO recombination on protein concentration, but rather a change in the relative proportion of the fast phase (high affinity tetramers) and the slow phase (lower affinity monomers), flash photolysis kinetics of CO in solution of the mutated β chains were analyzed in terms of their propensity to exist in either the monomer or tetrameric forms. Figure 6 presents the kinetics of CO recombination for the β_{40} (C6) Arg \rightarrow Ala, Val, and Asp mutations. For the three variants, the CO recombination kinetics are shifted to more slow phase relative to the native β subunits, indicating a larger fraction of monomers. The effect of the Arg \rightarrow Asp mutation leads to the presence of almost 40% slow phase at 65 μM heme, i.e., twice as much as for the Ala or Val mutations and four times the percentage found in solutions of normal β chains.

Figure 7 presents the CO recombination kinetics for the β_{40} Arg \rightarrow Ala mutant before and after addition of 1 mM IHP. Clearly, IHP increases the percentage of slow phase,

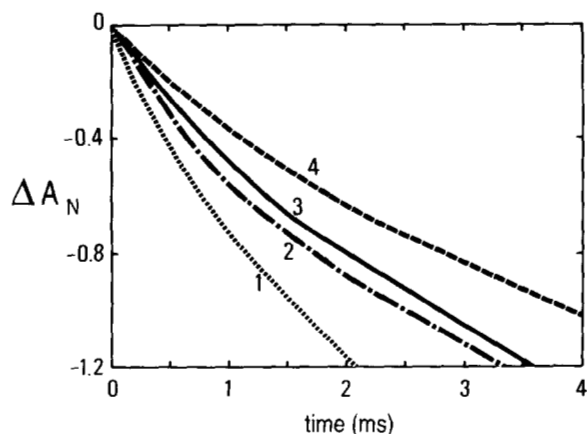


Fig. 6. Bimolecular recombination kinetics of CO to: (1) native β_4 tetramer (β_{40} Arg) and mutated β_4 tetramers; (2) Arg \rightarrow Val; (3) Arg \rightarrow Ala; and (4) Arg \rightarrow Asp. Conditions were 0.1 M phosphate buffer, pH 7, at 25 $^{\circ}\text{C}$. Heme concentration was 100 μM , and [CO] was 0.1 atm. At the heme concentration used here, the ratio of the slow to fast rates was 0.15 for the native β_4 tetramer and about 0.65 for the β_4 40 Arg \rightarrow Asp mutant, indicating an increased amount of monomer in the latter.

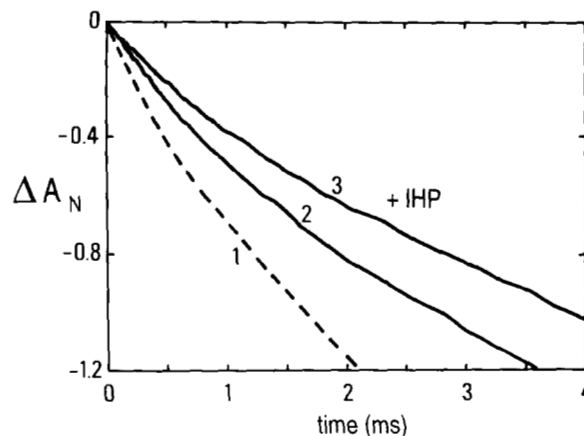


Fig. 7. Recombination kinetics of CO to: (1) native β_4 ; (2) β_4 Arg \rightarrow Ala; and (3) β_4 Arg \rightarrow Ala + 0.1 mM IHP. Conditions were 0.1 M phosphate buffer, pH 7, at 25 $^{\circ}\text{C}$. Heme concentration was 50 μM , and [CO] was 0.1 atm.

indicative of the presence of more monomers. At 100 μM concentration of β chains, IHP has no observable effect on the kinetics of normal β chains; at low heme concentrations ($<0.5 \mu\text{M}$), IHP favors β tetramers over monomers (the overall rate is faster). Similar observations were obtained for the β Arg \rightarrow Val or Asp mutants. These results demonstrate that any change in the residue side chain at the β_{40} position leads to instability of the tetrameric form which, if also present in the heterologous tetramers, may well explain the abnormal functional properties of these mutants. Interestingly, the measurements of the CO recombination kinetics for the β_{101} Glu \rightarrow Ala mutated subunit demonstrated a much larger proportion of the slow phase both in the absence and in the presence of IHP (40% and 55%, respectively).

Model building of the allosteric interface in β_4 tetramers

In this study the modified residues occur at the $\alpha_1\beta_2$ interface; their interactions may be represented by the pairwise interactions across the interface, as indicated in Figure 8. This interface is in close proximity to the hemes and intimately involved in cooperative interactions. It is composed of residues from the C helix, the FG corner, the beginning of the G helix, and the C-terminal portion of the chains. As summarized in Figure 8A, 10 α chain and 10 β chain residues participate in the R-state. For the β_4 tetramer, this interface, presented in Figure 8B, parallels the structure of the interface of HbA for the R-state. According to our criteria, 11 β residues participate, one more than for the contribution of β chains to the corresponding interface in HbA. All but two of these residues (β_{98} Val and β_{100} Pro) also occur among the contributions of the β chains to the interface in HbA, but these

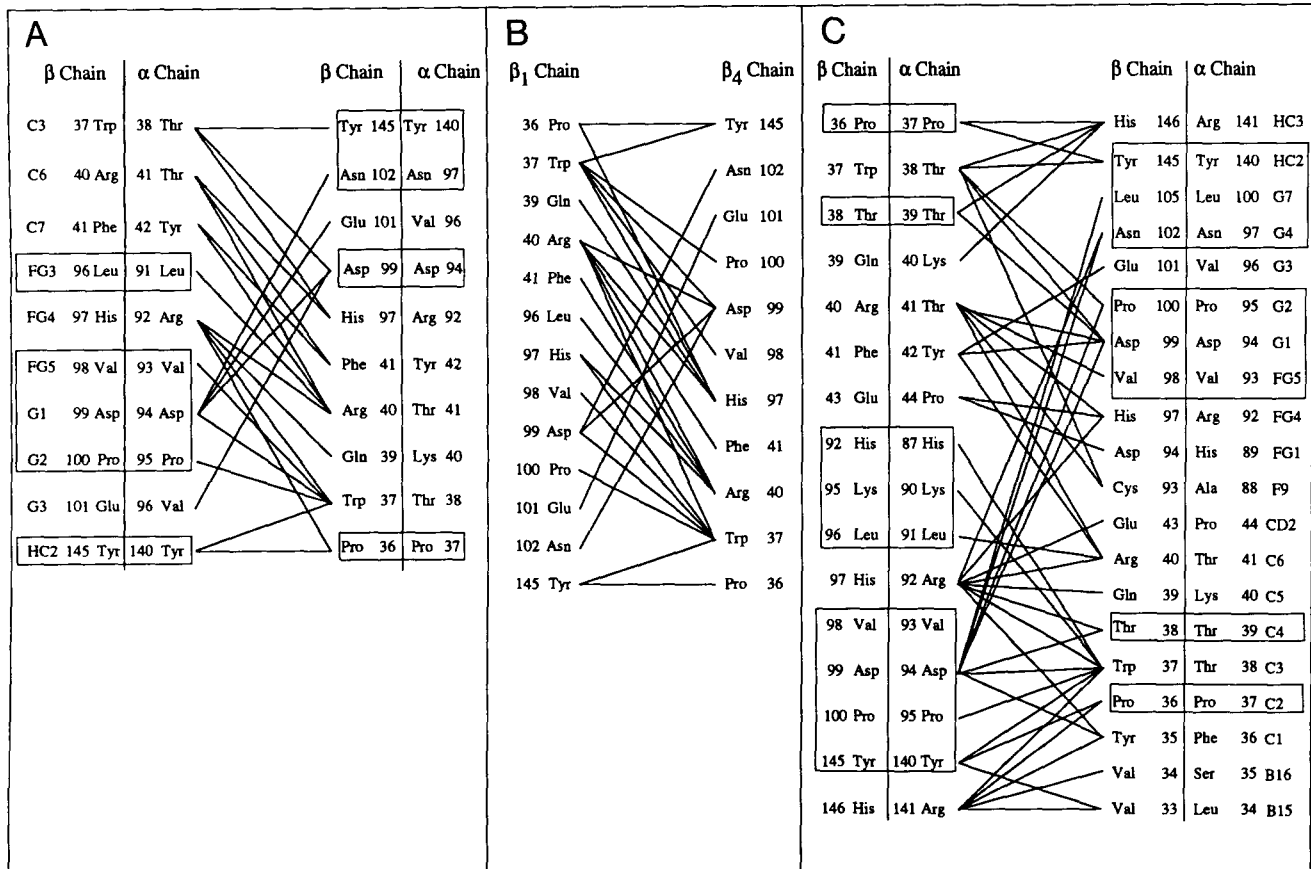


Fig. 8. Residues participating in the $\alpha_1\beta_2$ interface. **A:** HbA in the R-state. **B:** The β_4 tetramer. **C:** HbA in the T-state. Residues contributing to the interface as evaluated by energy criteria described in the text are indicated by connecting lines. For comparison, the corresponding residue of the other class of chains is indicated by the lists outside the vertical lines for HbA in parts A and C. Boxes surround the residues that are identical for both the corresponding positions of both α and β chains. The residues presented here agree with the assignments of Fermi and Perutz (1981) for the R-state, with the following exceptions. They assign $\alpha 97$ Asn and $\beta 43$ residues to the interface. These residues do not participate by our criteria, whereas we assign four residues to the interface that were not noted by Fermi and Perutz: $\alpha 91$ Leu, $\alpha 93$ Val, $\beta 36$ Pro, and $\beta 145$ Tyr. For the T-state they did not find the α chain residues 39 Thr, 87 His, 90 Lys, and 93 Val at the interface, nor the β chain residues 38 Thr, 39 Gln, 93 Cys, and 94 Asp. In addition, they included the following residues that were not found at the interface by our methods: $\alpha 86$ Ala, $\alpha 96$ Val, $\alpha 97$ Asn, and $\beta 41$ Phe.

two residues are at positions where the corresponding residues of the α chains participate to the interface for HbA. In addition, $\beta 39$ Gln, identified as participating in the contact for HbA, was not found in the contact for β_4 tetramer.

For HbA, structural differences between R and T are extensive, since the allosteric transition concerns mainly this interface. The residues identified by our energy criteria as participating in the interface for Hb are indicated in Figure 8C. The interface is clearly much more extensive for the T-state than for the R-state, involving 16 α residues and 20 β residues, compared to the R-state with each chain contributing only 10 residues. Among the T-state residues at the interface are all of the residues that participate in the R-state except $\alpha 96$ Val and $\beta 41$ Phe. Moreover, there are 7 additional residues for the α and 11 additional residues for the β chain that change the

character of the interface considerably. The additional residues involve principally the C-terminal positions of both chains, as well as portions of the C and F helices.

The allosteric transition involves reorientation of the β chains such that there is a crossing between the C helix and the FG corner. For example, $\alpha 42$ Tyr moves from a position in the R centered about a contact with $\beta 40$ Arg and $\beta 41$ Phe of the C helix to a position in T that, while maintaining a contact with $\beta 40$ Arg of the C helix, extends the contacts to the G helices and residues $\beta 99$ Asp and $\beta 101$ Glu. As revealed by the data presented here, modifications of the key residues $\beta 40$ Arg, $\beta 99$ Asp, and $\beta 101$ Glu invariably reduce the stability of the T-state. These residues are also clearly implicated in the stability of the tetramers (Turner et al., 1992), since the various mutations tested favor dissociation to monomeric β chains.

Conclusions

All mutations at the $\alpha_1\beta_2$ interface that have been studied here for either heterologous or homologous β tetramers result in the weakening or the complete disruption of the tetramer assembly. This interface is so precisely tailored for maintaining the assembly between $\alpha\beta$ dimers in HbA that any change in the side chains of residues 40 (C6), 99 (G1), and 101 (G3) involved in this interface results in increased R-state behavior (low or no cooperativity, increased ligand affinity), likely due both to the destabilization of the quaternary T-state and to the enhancement of dimer formation. This is suggested by the partial restoration of the functional properties of these Hbs on addition of organophosphate effectors.

These results also suggest that the stable form is the R-state of the β_4 tetramer, whether in the oxy or deoxy form, supporting the view that the peculiar behavior of the homologous tetramer is related to the instability of the quaternary T-state conformation, as also suggested by Arnone et al. (1982) from the analyses of the three-dimensional structure of the CO liganded β_4 tetramer. More detailed studies and calculations are necessary to determine the cause of this large T-state instability of the deoxy β_4 tetramers. The results presented above also raise the question of how such a precisely tailored allosteric interface either in the hetero- or homotetramers has been built from point mutations in the α and ancestral non- α chains during the evolutionary processes.

Materials and methods

HbA was prepared from fresh red blood cell hemolysates by chromatography on a DEAE-Sephadex column. The purity of the solute was verified by isoelectric focusing, showing a single band migrating at $pI = 6.95$. The Hb was further stripped of remaining contaminants on an ion-exchange column consisting of ion-retardation resin AG11A8 and mixed-bed exchange resin AG501X8-D from Bio-Rad. Hb was concentrated under vacuum to 2 mM heme and stored in the oxy form in liquid nitrogen until use. The methemoglobin content of the stock solution was less than 2%. The β^{PMB} subunits were prepared from saturated CO-HbA using the method of Bucci and Fronticelli (1965), and the free sulfhydryl groups were regenerated using 3 mM dithiothreitol. The β subunits were further purified twice on a DEAE-Sephadex column to remove any unregenerated components. The purity of the β^{SH} solution was estimated by isoelectric focusing and spectrophotometric criteria. After extensive dialysis against a 10 mM phosphate buffer at pH 7 and vacuum concentration, the free β chains were stored under 1 atm CO at 4 °C until use. Under these conditions, no degradation of the isolated subunits was observed during storage.

Expression of human β chains in *E. coli*

The β -globin chains were synthesized by using the expression vector pAT PrcIIFX β . This vector directs the synthesis of fusion protein CIIFX β -globin under the control of λ Pr promoter. *E. coli* strain CAG 1139, harboring pAT PrcIIFX β , was grown at 30 °C in M9 medium containing 2 g of glucose, 20 g of yeast extract, and 0.5 g of vitamin B₁ with 10 mg tetracycline per liter.

Synthesis of the cIIFX β -globin fusion protein was induced by inactivation of the temperature-sensitive repressor cI857 at 42 °C. The cells were harvested after 3–4 h incubation. The protein was extracted, purified, and cleaved with bovine coagulation factor Xa to liberate the β -globin (Nagai & Thogersen, 1987). The β_4 homotetramers were reconstituted in the presence of cyanhemine under 1 atm CO. Reconstitution of tetrameric heterotetramers ($\alpha_2\beta_2$) was carried out in the presence of CO-saturated native α chains. The reconstituted tetramers were reduced with sodium dithionite in the presence of CO and purified by ion-exchange chromatography on CM-cellulose and DEAE-Sephacel columns. Both types of Hb solutions were concentrated under vacuum (1–2 mM heme) and stored under 1 atm CO in the cold. The purity of the protein solutions was verified by isoelectric focusing and by recording visible absorption spectra. For equilibrium oxygen binding studies, the CO saturated Hb solutions were decarboxylated under a stream of pure O₂ and intense light in ice water for 1 h. Complete CO replacement by oxygen was verified from the visible absorption spectra. The equilibrium between tetramers, dimers, and monomers was studied using high performance size-exclusion chromatography, as described by Baudin-Chich et al. (1988). The experiments were performed in 0.1 M phosphate buffer, pH 7.5, and using a Lichrospher Diol Si 200 column.

Spectrophotometric studies

Static absorption spectra of the hetero- and homotetramers at a concentration of 100–150 μM on a heme basis were recorded with an SLM-Aminco DW 2000 spectrophotometer. The solutions were 100 mM NaCl, 50 mM Tris buffer, 1 mM EDTA, pH 7.2, at ambient temperature. They were prepared in glass tonometers to which an optical cuvette (0.2 cm pathlength) was attached. The concentration of the solutions was calculated from the absorbance of the CO component, taking an extinction coefficient $\epsilon_{540\text{nm}} = 14.3 \text{ mM}^{-1} \text{ cm}^{-1}$ (Zijlstra et al., 1991) for both the hetero- and homotetramers. In a typical experiment, the static spectrum of the CO component under 1 atm CO was first recorded. The sample was then decarboxylated by intense illumination under a stream of oxygen to obtain the oxy spectra. The two solutions of HbA and β_4 tetramer were deoxygenated under a stream of humidified argon. Traces of sodium dithionite

(<1% w/w) were added to remove any remaining oxygen, and the deoxy spectra were recorded. Finally, the sample was equilibrated under 1 atm CO, and a last CO spectrum was recorded and compared to the initial CO spectrum to verify the absence of hemoglobin denaturation. Difference spectra were calculated as deoxy (or CO) HbA – deoxy (or CO) β_4 tetramer. The same procedure was used for the recording of the weak absorption band at 760 nm that is present in only deoxy hemes and is commonly referred to as band III. The deoxy spectra shown in Figure 2 have been calculated after subtraction of the small CO absorbance spectra.

Fluorescence studies were performed on 10 μ M heme solutions, 10 mM phosphate buffer, pH 7.0, using an SLM 8000 spectrofluorometer. Optical cuvettes were 4 \times 10 mm, with excitation at 280 nm along the 10-mm axis. Emission spectra were recorded for both the buffer and the liganded Hb samples. The data were analyzed after subtraction of the buffer spectrum. No significant differences were observed relative to the native Hb solutions, indicating correct refolding of the recombinant Hbs.

Functional studies

Oxygen equilibrium studies were performed only for native and recombinant heterotetramers by a continuous recording method using a Hemox Analyzer (TCS-Medical Products Co., Huntington Valley, Pennsylvania) and analyzed as previously described (Kister et al., 1987). Typical samples were 60 μ M heme, 100 mM NaCl in 50 mM bisTris buffer, pH 7.2, at 25 °C. When necessary, buffered aliquots of DPG or of IHP were added in large molar excess to the tetramer concentration. Data were analyzed according to the formalism of the two-state allosteric model (Monod et al., 1965).

Kinetics of CO recombination after flash photolysis

The bimolecular recombination rates (k_{on}) were measured after photodissociation by a 10-ns laser pulse delivering 160 mJ at 532 nm (Quantel YAG laser, France). Samples were 1–100 μ M in heme in 1- or 2-mm optical cuvettes, with observation at 436 nm (Marden et al., 1988). Measurements were made at 1 and 0.1 atm CO at different levels of dissociation (10–50%). For solutions of β chains, small amounts of sodium dithionite were added shortly before the experiment in order to remove any trace of oxygen. Hb concentrations were determined from the extinction coefficients of CO Hb in the visible region of the spectrum. CO concentrations for the analyses of the kinetic data were based on Henry's law coefficient of 1 mM/atm at 20 °C. Curve fitting procedures for the calculation of the CO recombination rates were performed as described in Marden et al. (1988).

Model building

Computer models to aid in the design and interpretation of the investigations on β chain mutants were constructed using the BRUGEL program package (Delhaise et al., 1984) on the basis of the structures of liganded (Shaanan, 1983) and unliganded (Fermi et al., 1984) human hemoglobin, using the coordinates deposited in the Protein Data Bank and the coordinates of Hb H kindly provided by Dr. A. Arnone (Arnone et al., 1982). Energy minimizations were performed on all the structures examined until a root mean square of the derivative of the energy function of 0.1 kcal/mol \cdot Å was achieved. Residues at the opposite sides of an interface were considered to interact if the sum of the pairwise contacts between them contributes at least 1% of the van der Waals potential between the two subunits (Schaad, 1991). A contact was then indicated by a line between the two residues (Fig. 8).

Acknowledgments

This work was supported by funds from Inserm, the Faculté de Médecine Paris-Sud, l'Air Liquide Co (Fondation pour la Recherche Médicale), the Direction des Recherches et Techniques (contract 89/245), and the Swiss National Science Foundation. We also acknowledge the valuable technical help of B. Bohn, T. Gorsky, and V. Dodon.

References

- Antonini, E. & Brunori, M. (1971). *Hemoglobin and Myoglobin in Their Interactions with Ligands* (Neuberger, A. & Tatum, E.L., Eds.). North Holland Publishing Co., Amsterdam.
- Arnone, A. & Briley, P.D. (1978). Location of the heme iron atoms and characterization of the quaternary structure of the carbonmonoxy- β_4 tetramer. In *Biochemical and Clinical Aspects of Hemoglobin Abnormalities* (Caughy, W.S., Ed.), pp. 93–105. Academic Press, New York.
- Arnone, A., Briley, P.D., Rogers, P.H., & Hendrickson, W.A. (1982). Structure–function relationships in carbonmonoxy β_4 hemoglobin. In *Hemoglobin and Oxygen Binding* (Ho, C., Ed.), pp. 127–133. Elsevier-North Holland Inc., Amsterdam.
- Baudin-Chich, V., Marden, M., & Wajcman, H. (1988). Investigation of the tetramer–dimer equilibrium in hemoglobin solutions by high performance size exclusion chromatography on a diol column. *J. Chromatogr.* 437, 193–201.
- Bucci, E. & Fronticelli, C. (1965). A new method for the preparation of α and β subunits of human hemoglobin. *J. Biol. Chem.* 240, 551–553.
- Campbell, B.F., Chance, M.R., & Friedman, J.M. (1987). Linkage of functional and structural heterogeneity in proteins: Dynamic hole burning in carboxymyoglobin. *Science* 238, 373–375.
- Delhaise, P., Bardiaux, M., & Wodak, S. (1984). Interactive computer animation of macromolecules. *J. Mol. Graphics* 2, 103–106.
- Dickerson, R.E. & Geis, I. (1983). *Hemoglobin: Structure, Function, Evolution, and Pathology*. The Benjamin Cummings Publishing Co, Menlo Park, California.
- Dunn, R.C. & Simon J.D. (1991). Picosecond study of the near infrared absorption band of hemoglobin after photolysis of carbonmonoxyhemoglobin. *Biophys. J.* 60, 884–885.
- Eaton, W.A., Hanson, L.K., Stephens, P.J., Sutherland, J.C., & Dunn, J.B.R. (1978). Optical spectra of oxy and deoxyhemoglobin. *J. Am. Chem. Soc.* 100, 4991–5003.
- Fermi, G. & Perutz, M.F. (1981). *Atlas of Molecular Structures in Biology. 2: Haemoglobin and Myoglobin*. Clarendon Press, Oxford, UK.

- Fermi, G., Perutz, M.F., Shaanan, B., & Fourme, R. (1984). The crystal structure of human deoxyhemoglobin at 1.74 Å. *J. Mol. Biol.* *175*, 159–174.
- Friedman, J.M. (1985). Structure, dynamics and reactivity in hemoglobin. *Science* *228*, 1273–1280.
- International Hemoglobin Information Center. (1992). Hemoglobin variant list. *Hemoglobin* *16*, 127–213.
- Kister, J., Poyart, C., & Edelstein, S.J. (1987). Oxygen–organophosphate linkage in hemoglobin A. The double hump effect. *Biophys. J.* *52*, 527–535.
- Kitagawa, T. (1992). Investigation of higher order structures of proteins by ultraviolet resonance Raman spectroscopy. *Progr. Biophys. Mol. Biol.* *58*, 1–18.
- Kurtz, A., & Bauer, C. (1978). The oxygen affinity of hemoglobin β^{SH} chains is concentration dependent. *Biochem. Biophys. Res. Commun.* *84*, 852–857.
- Kurtz, A., Rollema, H.S., & Bauer, C. (1981). Heterotropic interactions in monomeric β^{SH} chains from human hemoglobin. *Arch. Biochem. Biophys.* *210*, 200–203.
- Marden, M.C., Kister, J., Bohn, B., & Poyart, C. (1988). T-state hemoglobin with four ligands bound. *Biochemistry* *27*, 1659–1664.
- Martin, J.L., Migus, A., Poyart, C., Lecarpentier, Y., Astier, R., & Antonetti, A. (1983). Femtosecond photolysis of CO-ligated protoheme and hemoproteins: Appearance of deoxy species with a 350-fsec time constant. *Proc. Natl. Acad. Sci. USA* *80*, 173–177.
- Monod, J., Wyman, J., & Changeux, J.P. (1965). On the nature of the allosteric transition: A plausible model. *J. Mol. Biol.* *12*, 88–118.
- Moo-Penn, W.F., Johnson, M.H., Bechtel, C., Jue, D.L., Therrel, B.L., & Schmidt, R.M. (1977). Hemoglobins Austin and Waco: Two hemoglobins with substitutions in the $\alpha_1\beta_2$ contact region. *Arch. Biochem. Biophys.* *179*, 86–94.
- Mrad, A., Kister, J., Feo, C., Poyart, C., Kastally, R., Blibech, R., Galacteros, F., & Wajcman, H. (1989). Hemoglobin Athens-Georgia [$\alpha_2\beta_2$ 40 (C6) Arg → Lys] in association with β^0 -thalassemia in Tunisia. *Am. J. Hematol.* *32*, 117–122.
- Nagai, K., & Thogersen, H.C. (1987). Synthesis and sequence specific proteolysis of hybrid proteins produced in *Escherichia coli*. *Methods Enzymol.* *153*, 461–481.
- Perutz, M.F. (1970). Stereochemistry of cooperative effects in hemoglobin. *Nature* *228*, 726–734.
- Perutz, M.F., Fermi, G., Luisi, B., Shaanan, B., & Liddington, R.C. (1987). Stereochemistry of cooperative mechanisms in hemoglobin. *Acc. Chem. Res.* *20*, 309–321.
- Perutz, M.F., Ladner, J.E., Simon, S.R., & Chien Ho. (1974). Influence of globin structure on the state of the heme. I. Human deoxy-hemoglobin. *Biochemistry* *13*, 2163–2173.
- Petrich, J.W., Lambry, J.C., Kuczera, K., Karplus, M., Poyart, C., & Martin, J.L. (1991). Ligand binding and protein relaxation in heme proteins: A room temperature analysis of NO geminate recombination. *Biochemistry* *30*, 3975–3997.
- Philo, J.S., Adams, M.L., & Shuster, T.M. (1981). Association-dependent absorption spectra of oxyhemoglobin A and its subunits. *J. Biol. Chem.* *256*, 7917–7924.
- Philo, J.S., Lary, J.W., & Shuster, T.M. (1988). Quaternary interactions in hemoglobin β subunit tetramers. *J. Biol. Chem.* *263*, 682–689.
- Sawicki, C.A., & Gibson, Q.H. (1976). Quaternary conformational changes in human hemoglobin studied by laser photolysis of carbon-monooxyhemoglobin. *J. Biol. Chem.* *251*, 1533–1542.
- Schaad, O. (1991). Modélisation moléculaire de deux protéines des globules rouges humains: L'hémoglobine et la bisphosphoglycerate mutase. Ph.D. Thesis, University of Geneva, Geneva.
- Shaanan, B. (1983). Structure of human oxyhemoglobin at 2.1 Å resolution. *J. Mol. Biol.* *171*, 31–59.
- Shih, D.T.-B., Jones, R.T., Imai, K., & Tyuma, I. (1985). Involvement of Glu (101) β in the function of hemoglobin. *J. Biol. Chem.* *260*, 5919–5924.
- Tainsky, M., & Edelstein, S.J. (1973). Enhanced quaternary stability of β_4 hemoglobin in 2 M-sodium chloride. *J. Mol. Biol.* *75*, 735–739.
- Turci, S.M., & McDonald, M.J. (1983). The effect of pH on the rate of dissociation of oxygenated beta chain tetramer of hemoglobin A. *Biochem. Biophys. Res. Commun.* *111*, 55–60.
- Turner, G.J., Galacteros, F., Doyle, M.L., Hedlund, B., Pettigrew, D.W., Turner, B.W., Smith, F.R., Moo-Penn, W., Rucknagel, D.L., & Ackers, G.K. (1992). Mutagenic dissection of hemoglobin cooperativity: Effects of amino acid alteration on subunit assembly of oxy and deoxy tetramers. *Proteins Struct. Funct. Genet.* *14*, 333–350.
- Valdes, R., & Ackers, G.K. (1977). Thermodynamic studies on subunit assembly in human hemoglobin self-association (α^{SH} and β^{SH}): Determination of stoichiometries and equilibrium constants as a function of temperature. *J. Biol. Chem.* *252*, 2926–2929.
- Valdes, R., & Ackers, G.K. (1978). Self-association of hemoglobin β^{SH} chains is linked to oxygenation. *Proc. Natl. Acad. Sci. USA* *75*, 311–314.
- Zijlstra, W.G., Buursma, A., & Meeuwse-van der Roest, W.P. (1991). Absorption spectra of human fetal and adult oxyhemoglobin, deoxyhemoglobin, carboxyhemoglobin, and methemoglobin. *Clin. Chem.* *37*, 1633–1638.